

RSC Advances



This is an *Accepted Manuscript*, which has been through the Royal Society of Chemistry peer review process and has been accepted for publication.

Accepted Manuscripts are published online shortly after acceptance, before technical editing, formatting and proof reading. Using this free service, authors can make their results available to the community, in citable form, before we publish the edited article. This *Accepted Manuscript* will be replaced by the edited, formatted and paginated article as soon as this is available.

You can find more information about *Accepted Manuscripts* in the [Information for Authors](#).

Please note that technical editing may introduce minor changes to the text and/or graphics, which may alter content. The journal's standard [Terms & Conditions](#) and the [Ethical guidelines](#) still apply. In no event shall the Royal Society of Chemistry be held responsible for any errors or omissions in this *Accepted Manuscript* or any consequences arising from the use of any information it contains.

Poromechanical modeling of moisture induced swelling anisotropy in cellular tissues of softwoods

Ahmad Rafsanjani,^{*a,b,c} Dominique Derome,^b and Jan Carmeliet^{b,c}

Date: November 27, 2014

Experimental studies reveal that softwoods exhibit different swelling patterns at the cellular scale depending on the position of the tracheid cells within the growth ring. Thin-walled earlywood cells show anisotropic swelling behavior while the swelling of thick-walled bulky latewood cells is generally isotropic. A poromechanical model is developed to explore the anisotropic swelling behavior of softwoods at the cellular scale. The general description for the macroscopically observable free swelling strain of cellular tissues is derived by upscaling the constitutive equations of a double porosity medium which is found to be dependent on stiffness, Biot coefficient, Biot modulus and the geometry of the cells. The effective poroelastic constants of earlywood and latewood cells are computed from a periodic honeycomb unit cell by means of an efficient finite-element-based computational upscaling scheme. The estimated swelling coefficients compare well with experimental measurements. It is found that the anisotropy in swelling behavior of wood cells can be related to the anisotropy of elastic properties at the cell wall level and the geometry of the cells. The proposed poromechanical model provides a physically relevant description of swelling behavior which originates from the coupled interaction of water and solid phases within the porous cell walls of softwoods.

Introduction

Many biological tissues are essentially porous with a cellular microstructure which provides them with low density and high strength¹. Despite the considerable efforts devoted to the study of the mechanical behavior of cellular solids², little is known about how they behave in different environmental conditions. Softwood (wood of coniferous trees, e.g. cedars, Douglas firs, pines, spruces, and yews) is a natural hierarchical cellular material that undergoes anisotropic deformations when the humidity of the environment changes. It swells during wetting and shrinks upon drying^{3,4}. Hence, it is an interesting model material for studying the interaction of cellular materials with moisture. In temperate climate regions, tree growth occurs in the warm season, resulting in a mesoscale feature called growth ring (Fig. 1a) in which the thin-walled earlywood cells (grown in spring) with large lumens gradually change to bulky thick-walled latewood cells (grown in summer) with small lumens (Fig. 1b). Experimental results show that, in the plane transverse to the cells, earlywood cells swell anisotropically while the swelling behavior of latewood is almost isotropic^{5,6}.

The moisture induced deformation in wood originates from

the sub-cellular scale and is substantially influenced by the hierarchical structure of the material⁷. In softwoods, two main groups of porosities can be distinguished (Fig. 1c). Lumens are large pores of typical diameter of a few to hundred microns. Within the lumens, water is present in liquid or vapor phase and it is known that it does not participate in the moisture induced deformation in wood⁴. The second group of pores in wood are cell wall porosities which range in size from 5nm down to the level of single water molecules bound to hydrophilic sites of the wood polymers⁸. Thus, within the hygroscopic range, sorption of water occurs only at the cell wall level where the polar water molecules bind with hydrogen bonds to the hydroxyl sites of the polar molecules of wood polymers. Except for crystalline cellulose, all wood polymers demonstrate, to different extent, an affinity for water. In the dry state, the cell wall has a low porosity where water molecules can nevertheless find available sorption sites. For further sorption to take place, i.e. above 2-3% moisture content, the creation of new porosity by the displacement of molecules is required. Consequently, sorption of water molecules in between the hydrophilic molecules pushes the constituents apart which implies that within the hygroscopic range, the cell walls can be considered to be constantly filled with water⁹.

In literature, moisture induced swelling of wood is usually modeled by thermal expansion analogy in the framework of hydroelasticity^{10,11}. Based on this approach, swelling and stiffness of the material are treated as two uncoupled properties neglecting that the swelling behavior originates from the interaction of moisture and solid phases at the lower scales

^a McGill University, Mechanical Engineering Department, 817 Sherbrooke Street West, Montreal, QC, H3A 0C3, Canada

^b Swiss Federal Laboratories for Materials Science and Technology, EMPA, Laboratory for Building Science and Technology, Ueberlandstrasse 129, CH-8600 Dübendorf, Switzerland.

^c Swiss Federal Institute of Technology, ETH Zurich, Chair of Building Physics, Stefano-Frascini-Platz 5, CH-8093 Zurich, Switzerland.

* Corresponding author E-mail: ahmad.rafsanjani@mcgill.ca

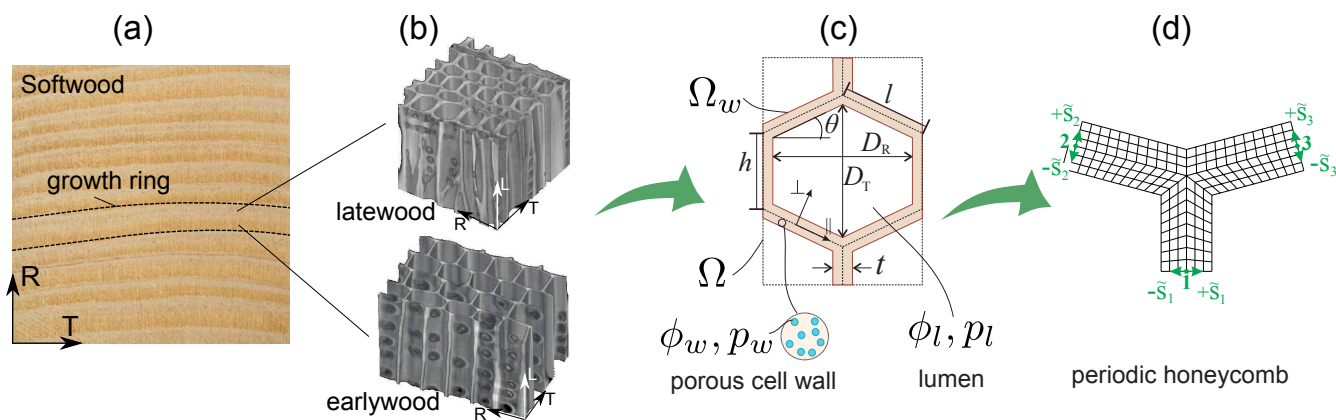


Fig. 1 (a) Cross section of a Norway spruce softwood sample and the indication of a growth ring. (b) The underlying latewood and earlywood cellular tissues of Norway spruce acquired by phase contrast synchrotron X-ray micro-computed tomography where R, T and L correspond to the anatomical directions of wood. (c) Double porosity honeycomb unit cell model used in the proposed poromechanical model where porosity manifests itself at two scales, i.e. lumens and cell wall porosity and (d) a quarter of a periodic honeycomb unit cell is discretized for finite element simulations.

and is coupled to moisture dependent mechanical properties. In contrast, poromechanics proposes a fully coupled approach for exploring the fluid and solid interaction in the material^{12,13}. Using analytical homogenization schemes, Bader *et al.*¹⁴ developed a multiscale model to predict the poroelastic properties of softwoods at different hierarchical levels. Looking at the swelling behavior, Lemarchand *et al.*¹⁵ investigated the expansive reactions in chemoelastic concrete based on an analytical micro-poromechanics model by bridging the scale from the local chemo-mechanical mechanisms to the macroscopically observable stress-free expansion. Carmeliet *et al.*¹⁶ proposed a nonlinear poroelastic constitutive model for wood, an unsaturated porous material, based on a higher order formulation of free energy including mechanical and moisture contributions and the coupling between moisture and mechanics. The nonlinear poroelastic material properties were determined from mechanical testing at different moisture content and free swelling/sorption tests. Rey and Vandamme¹⁷ studied the shrinkage and stiffening behavior of cellulose sponge upon drying using a double porosity poromechanical model where the large pores are filled by air and the small pores are saturated with water.

Here we develop a multiscale poromechanical model for the swelling behavior of softwood at cellular scale. While the actual microstructure of wood cells is far more complex, our model is intended to measure the respective role of structural and mechanical features of the cellular tissues of softwoods using a simplified poromechanical model in order to elucidate what is responsible for the swelling behavior of softwoods at higher hierarchical levels. In particular, we show how the swelling anisotropy can emerge at cellular scale from moisture-solid interactions at the cell wall level based on a

double-porosity poromechanical description of the underlying physical phenomena. Based on the simulation results, we aim to explain why, despite the moisture dependence of the stiffness properties of softwood, the swelling varies linearly with moisture content within the hygroscopic range. The proposed approach allows bridging the scales from the anisotropic poroelastic behavior of porous cell walls to the macroscopic free swelling of softwood at cellular scale.

Poromechanical model for softwood tissues

Constitutive equations

The cellular tissue of softwood can be considered as a double porosity material where the porosity manifests itself at two scales, i.e. lumens (denoted with l) and cell wall porosity (denoted with w). The porosity of the lumens ϕ_l which are large pores at the cellular scale is defined as the ratio of the volume of the lumens to that of the cells whereas the cell wall porosity ϕ_w is defined as the volume of the small pores within the cell wall to the cell wall volume. The poroelastic state equations for a double porosity material read¹⁸:

$$\sigma_{ij} = C_{ijkl}\epsilon_{kl} - b_{ij}^w p_w - b_{ij}^l p_l \quad (1)$$

$$\phi_w - \phi_w^0 = b_{ij}^w \epsilon_{ij} + \frac{p_w}{N_{ww}} + \frac{p_l}{N_{wl}} \quad (2)$$

$$\phi_l - \phi_l^0 = b_{ij}^l \epsilon_{ij} + \frac{p_w}{N_{wl}} + \frac{p_l}{N_{ll}} \quad (3)$$

where σ_{ij} is the stress tensor, ϵ_{ij} is the strain tensor, p_w is the pressure of the fluid prevailing in the cell walls with porosity

ϕ_w . The pressure of the fluid inside lumens is p_l and the porosity of the lumens is ϕ_l . The fourth-order stiffness tensor of the cellular tissue is C_{ijkl} . The second-order Biot coefficient tensors corresponding to cell wall porosities and lumens are b_{ij}^w and b_{ij}^l , respectively and N_{ww} , N_{wl} and N_{ll} are the Biot moduli of the system.

We note that all poroelastic properties are in general dependent on the independent variables strain and liquid pressures in wall and lumen. In this paper, as explained further in more detail, we will assume that stiffness, Biot coefficients and Biot moduli are dependent on moisture content. All the variables are Lagrangian variables which are defined with respect to the reference state at atmospheric pressure. In the following we limit our study to wood exposed to the changes in moisture content in the hygroscopic range. This means we assume the liquid in the cell wall is water, which is saturating the pore space, while the pore space in the lumen is not filled with liquid water, but by air at atmospheric pressure.

The water-filled cell wall porosity (denoted with ϕ_w) with respect to the cell wall volume Ω_w is expressed in terms of cell wall and lumen porosities as $\phi_w = \phi_w / (1 - \phi_l)$ and can be directly linked to mass of water by $m_f = \rho_f \phi_w \Omega_w$. In wood science, moisture content m is defined as the ratio of the mass of water m_w in the wood sample to the oven-dried mass $m_d = \rho_s (1 - \phi_w^0) \Omega_w^0$ of the sample as $m = m_f / m_d$ where ϕ_w^0 is the initial porosity of the cell wall and, ρ_f and ρ_s are densities of liquid water and the solid skeleton of the cell walls, respectively. Within the hygroscopic range, the pressure inside lumens is assumed to be equal to atmospheric pressure. Therefore, in the absence of external stresses ($\sigma_{ij} = 0$), the state equations (1-2) can be rewritten to express the free swelling strain ϵ_{ij}^0 in terms of poroelastic properties:

$$\epsilon_{ij}^0 = S_{ijkl}^u b_{kl}^w N_{ww} (\phi_w - \phi_{w0}) \quad (4)$$

where $S_{ijkl}^u = C_{ijkl}^u{}^{-1}$ is the undrained compliance tensor and $C_{ijkl}^u = C_{ijkl} + N_{ww} b_{ij}^w b_{kl}^w$ is the undrained stiffness tensor of the porous material. The free swelling strain defined by equation (4) can be related to the change of moisture content Δm resulting in the following relation:

$$\epsilon_{ij}^0 = \beta_{ij} \Delta m \quad (5)$$

where the equivalent second-order swelling coefficient tensor β_{ij} is defined as:

$$\beta_{ij} = S_{ijkl}^u b_{kl}^w N_{ww} (1 - \phi_l) (1 - \phi_w^0) \rho_s / \rho_f \quad (6)$$

The above equation shows that swelling coefficient is a function of stiffness, Biot coefficient and Biot modulus. In order to calculate the effective swelling coefficients of the cellular tissues of the softwood according to Eq. (6), as follows in the next subsections, we first need to find the poroelastic

properties of the cell walls as a function of the independent variables. Since this paper focuses on the determination of the swelling caused by a change in moisture content, we then determine the poroelastic properties as a function of moisture content using a finite-element based computational upscaling framework.

Poroelastic constants of cell wall

The poroelastic constants for an anisotropic porous material are usually expressed based on two fundamental assumptions of micro-homogeneity and micro-isotropy of the solid matrix¹⁹. The micro-homogeneity assumes that the solid matrix of the porous material is homogeneous at the pore scale while the material can be heterogeneous at the macroscopic scale. The micro-isotropy assumes that the solid constituent of the porous medium is isotropic at the pore level and the material anisotropy is of structural origin, mainly resulting from pore shape and orientation. By adopting these simplifications, and assuming that water is incompressible, the poroelastic constants of the cell wall can be defined as follows:

$$\tilde{b}_{ij}^w = \delta_{ij} - \frac{\tilde{C}_{ijkk}^w}{3K_s} \quad (7)$$

$$\frac{1}{\tilde{N}_w} = \frac{1}{K_s} \left[\left(1 - \frac{\tilde{C}_{iijj}^w}{9K_s} \right) - \phi_w^0 \right] \quad (8)$$

where the tilde symbol indicates that the poroelastic properties are measured at cell wall level. Above, δ_{ij} is the Kronecker delta, \tilde{C}_{ijkl}^w is the stiffness tensor of the porous cell wall and K_s is the bulk modulus of the solid matrix of the porous cell wall.

Upscaling from cell wall to cellular tissue

A finite-element-based computational upscaling scheme is used to compute the poroelastic constants of the double porosity model C_{ijkl} , b_{ij}^w and N_{ww} from the poroelastic properties of the anisotropic porous cell wall, i.e. \tilde{C}_{ijkl}^w , \tilde{b}_{ij}^w and \tilde{N}_w . Following the micromechanics of solids, the macroscopic behavior of cellular tissues are described by the behavior of an energetically equivalent homogenized continuum based on the Hill condition²⁰. Honeycomb unit cells with periodic boundary conditions are utilized. Due to the symmetry of the unit cells, the analysis of the original domain reduces to one quarter²¹. As shown in Fig. 1d, the deformation of the unit cell is controlled with three master nodes 1, 2 and 3. The periodic boundary conditions are imposed on the reduced unit cells through the constrained relation $\vec{x}(-\tilde{s}_q) + \vec{x}(\tilde{s}_q) = 2\vec{x}_q$ (for $q = 1, 2, 3$) where \tilde{s}_q denotes a local coordinate system centered on a master node and \vec{x}_q is the position vector of this

node. The displacement vectors of the master nodes are related to the macroscopic strain with $u_i^q = \varepsilon_{ij}x_j^q$. The application of the averaging theorem on σ_{ij} over Ω and the transformation from volume integrals to surface integrals for a periodic unit cell can be elaborated as follows:

$$\sigma_{ij} = \frac{1}{\Omega} \sum_{q=1,2,3} f_i^q x_j^q \quad (9)$$

where f^q is the reaction external force acting on the master node q . The stiffness tensor of honeycombs C_{ijkl} are computed with a computational upscaling procedure as described in detail by Rafsanjani *et al.*²². The poroelastic constants of the double porosity model b_{ij}^w and N_{ww} can be calculated computationally for a honeycomb unit cell where its macroscopic strain is constrained, i.e. $\varepsilon_{ij} = 0$, and the unit cell is subjected to a small change of pore pressure Δp_w . The cell wall Biot coefficient tensor b_{ij}^w is obtained by probing the change of the macroscopic stress in the unit cell from Eq. (9) through the poroelastic constitutive Eq. (1) as:

$$b_{ij}^w = - \left. \frac{\Delta \sigma_{ij}}{\Delta p_w} \right|_{\varepsilon_{ij}=0} \quad (10)$$

The Biot modulus N_{ww} can also be computed in the same experiment from Eq. (2):

$$N_{ww} = \left. \frac{\Delta p_w}{\Delta \phi_w} \right|_{\varepsilon_{ij}=0} \quad (11)$$

with $\Delta \phi_w = \frac{1}{\Omega} \int_{\Omega_w} (\phi_w - \phi_w^0) d\Omega$ which is determined from finite element simulations. The above constants are used in Eq. (6) to determine the swelling coefficient tensor of the cellular tissues of the softwood.

Results and Discussion

The proposed poromechanical model has been implemented in the scripting environment of the finite element package ABAQUS (Rising Sun Mills, Providence, RI, USA) and used to predict the swelling behavior of softwood at the cellular scale. The longitudinal dimensions of the wood cells are very large in comparison to radial and tangential directions and we confine the analysis to the cross-section of the material which is in a state of generalized plane strain. In these analyses, the cell wall was discretized using plane strain elements with pore pressure (CPE8P). The moisture dependency of the elastic properties of the wood cell wall is adopted from the micro-mechanical model developed by Qing and Mishnaevsky¹⁰. The transverse elastic Young's moduli (\tilde{E}_1^w and \tilde{E}_2^w) and the in-plane shear modulus (\tilde{G}_{12}^w) are shown in Fig. 2.

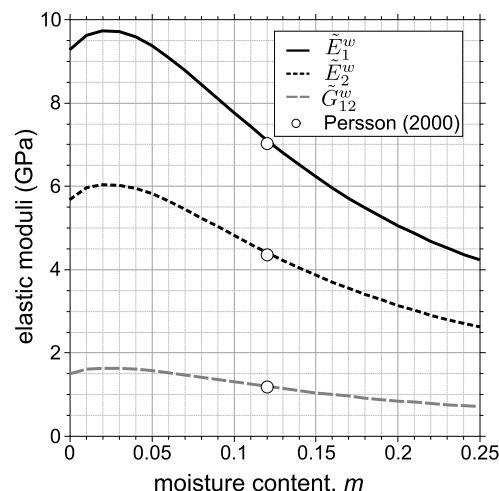


Fig. 2 Moisture dependent relationship of the transverse elastic Young's (\tilde{E}_1^w and \tilde{E}_2^w) and shear (\tilde{G}_{12}^w) moduli of the wood cell wall adopted from Qing and Mishnaevsky¹⁰ and used as input in the proposed model. The symbols show the transverse elastic properties which are adopted from the micromechanical model by Persson²³.

In the following, first, the overall validity of the work is established by comparing the results of the proposed poromechanical model with experimental data. Then, the poroelastic properties and swelling coefficients of earlywood and latewood cells are predicted and the influence of shape angle of the honeycomb unit cell on the effective swelling behavior is obtained. The key findings are finally discussed.

Comparison with experimental measurements

We compare the results of the proposed poromechanical model with experimental measurements. The experimental data consist of two sets (called A and B) of isolated earlywood (EW) and latewood (LW) tissues of Norway spruce softwood originating from two different wood sources. The moisture induced deformation of softwood tissues exposed to different relative humidity conditions are measured by high resolution phase contrast synchrotron X-ray tomography (TOMCAT beamline, Swiss Light Source, Paul Scherrer Institute, Villigen, Switzerland). The free swelling and shrinkage strains are determined by affine registration method⁵. The moisture content of the samples are measured by means of a dynamic vapor sorption (DVS) apparatus. Since a quasi linear relation between swelling and moisture content variation was found, the effective swelling coefficients of the samples are determined in radial and tangential directions from the slope of the strain curve plotted versus moisture content⁶.

The dimensions of the honeycomb unit cell (l , h , t and θ) are determined by correlating the lumens porosity ϕ_l and radial ($D_R = 2l \cos \theta - t$) and tangential ($D_T = h + 2l \sin \theta -$

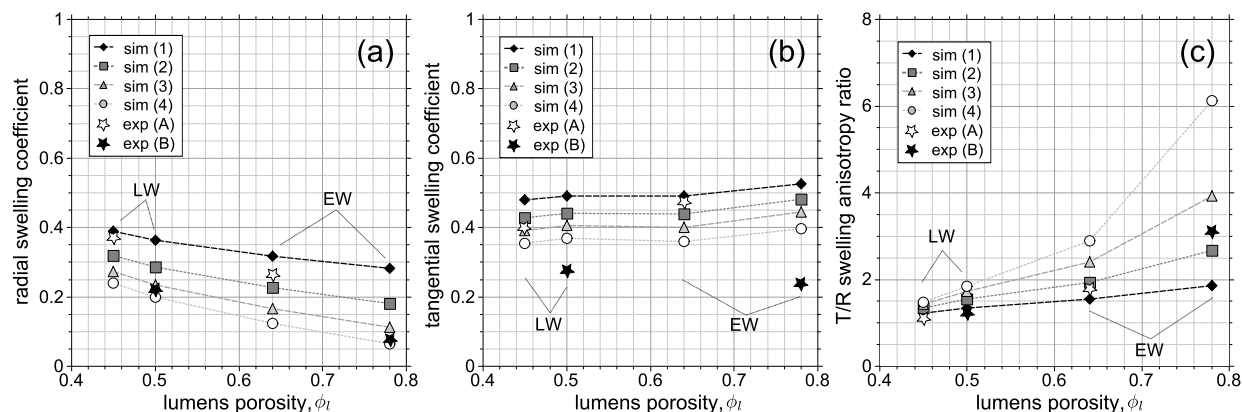


Fig. 3 Comparison of experimental measurements⁶ and simulation results of swelling coefficients of Norway spruce softwood tissues in (a) radial and (b) tangential directions and (c) the tangential to radial (T/R) swelling anisotropy ratio at different lumen porosity ϕ_l and moisture content $m = 0.12$. The simulations correspond to different elastic Young's moduli of the cell wall, \tilde{E}_1^w and \tilde{E}_2^w , as defined in Tab. 2.

Table 1 Geometrical parameters of the cellular tissues of softwood as defined in Fig. 1c (lumen porosity ϕ_l , unit cell dimensions h and l , cell wall thickness t and shape angle θ) adopted from experimental data^{5,6} and used as inputs in the poromechanical model.

wood tissue	ϕ_l	h (μm)	l (μm)	t (μm)	θ
EW_A	0.78	35	21	4.7	6°
EW_B	0.64	35	18	7.6	10°
LW_B	0.50	30	16	9.9	14°
LW_A	0.45	30	15	10.8	16°

$t \sec \theta$) diameters of unit cells to those of real wood cells as explained in Rafsanjani *et al.*²⁴. The geometrical properties of four cellular tissues corresponding to experimental data are summarized in Tab. 1. The elastic properties of the cell wall material are adopted from Persson²³ and presented in Tab. 2. In this table, directions 1, 2 and 3 are respectively equivalent to parallel (\parallel), perpendicular (\perp) and longitudinal (L) directions with respect to the cell wall as defined in Fig. 1c. Fig. 3a and b show the comparison between the experimental data and simulation results for effective swelling coefficients in radial and tangential directions. The two experimental datasets used a different source for the sample, thus it can be expected that the elastic properties of the cell walls for these two datasets are different. Therefore, the comparison is performed for a range of elastic Young's moduli in transverse plane by varying the anisotropy ratio $\tilde{E}_1^w/\tilde{E}_2^w$ from 1.75 to 10 while keeping all other elastic properties constant (referred to as sim (1), (2), (3) and (4) on Tab. 2 and Fig. 2). The density of the dry cell wall and water are $\rho_s = 1500 \text{ kg/m}^3$ and $\rho_f = 1000 \text{ kg/m}^3$, respectively.

Simulations show that the swelling coefficients in tangential direction are almost constant for earlywood (high porosity) and latewood (low porosity) tissues of both datasets while,

Table 2 Elastic properties of wood cell wall at moisture content $m = 0.12$ adopted from Persson²³. In this table, directions 1, 2 and 3 are respectively referring to parallel (\parallel), perpendicular (\perp) and longitudinal (L) directions with respect to the cell wall as defined in Fig. 1c.

Young's moduli (GPa)				Poisson's ratio	Shear moduli (GPa)	
sim	1	2	3	4		
$\tilde{E}_1^w =$	7	8	9	10	$\tilde{\nu}_{12}^w = 0.65$	$\tilde{G}_{12}^w = 1.1$
$\tilde{E}_2^w =$	4	3	2	1	$\tilde{\nu}_{13}^w = 0.11$	$\tilde{G}_{13}^w = 4.5$
$\tilde{E}_3^w =$	33				$\tilde{\nu}_{23}^w = 0.02$	$\tilde{G}_{23}^w = 2.3$

in radial direction, the swelling coefficient of earlywood is smaller than latewood. The swelling coefficients in both radial and tangential direction decrease by increasing the anisotropy ratio $\tilde{E}_1^w/\tilde{E}_2^w$. The corresponding swelling anisotropy ratio β_T/β_R is shown in Fig. 3c. The swelling anisotropy increases with the increase of porosity ϕ_l . This behavior has been successfully captured with the proposed poromechanical model. We also observed an increase of swelling anisotropy with the increase of lumen porosity and the Young's moduli ratio $\tilde{E}_1^w/\tilde{E}_2^w$ in the plane of the cell wall.

Swelling coefficients of earlywood and latewood cells

In this section, we use the proposed model to explore the swelling behavior of earlywood and latewood tissues. For this purpose, we consider the geometrical parameters of EW_B and LW_B in the rest of this article for parametric studies.

The Biot coefficients in radial ($b_R^w = b_{11}^w$) and tangential ($b_T^w = b_{22}^w$) directions, are computed as a function of moisture content m using Eq. (10) and the results are shown in Fig. 4a. The moisture dependency of elastic properties of the cell wall has a little influence on the Biot coefficients of cellular tissue

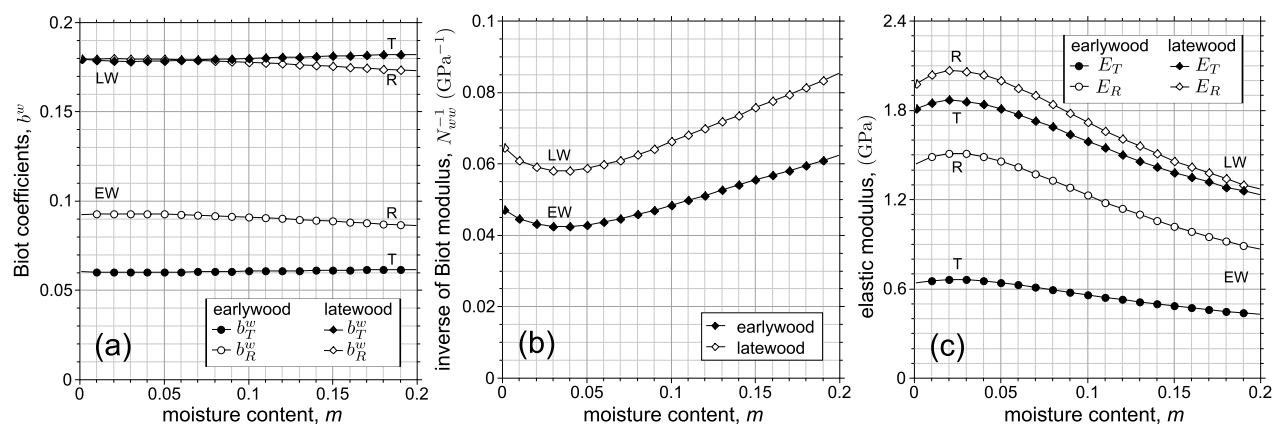


Fig. 4 Simulation results for moisture dependency of poroelastic properties of earlywood ($\phi_l = 0.64$) and latewood ($\phi_l = 0.45$) cells: (a) Biot coefficients b_R^w and b_T^w , (b) the inverse of Biot modulus N_{ww}^{-1} and (c) elastic Young's moduli E_R and E_T .

and both b_R^w and b_T^w are almost constant. In earlywood $b_R^w > b_T^w$ while in latewood $b_R^w \approx b_T^w$. The Biot coefficients at low lumen porosity (latewood) are larger than ones at high lumen porosity (earlywood). The Biot coefficient can be interpreted by the following experiment. Imagine the conditions where the external deformation of the wood cells is constrained and the cell walls are pressurized by the water they contain, then the Biot coefficient measures the transmitted pressure to the boundaries of the medium, also referred to as swelling pressure. The large Biot coefficient in latewood compared to earlywood means that the swelling pressure in latewood is larger than in earlywood which could be due to the thicker walls of latewood cells. In earlywood, the results show that the pressure that is transmitted from the water within the cell walls onto the radial boundaries of a constrained sample is larger than the one onto the tangential ones. In comparison to other porous materials, such as sandstones and rocks ($b \sim 0.7$), the Biot coefficients predicted for softwood cells are much smaller due to presence of large empty lumens.

The Biot moduli (N_{ww}) of earlywood and latewood cells are computed as a function of m using Eq. (11) and the inverse of the Biot moduli (N_{ww}^{-1}) are illustrated in Fig. 4b. The moisture dependency of the Biot modulus is similar to that of the elastic properties of the cell wall. The inverse of the Biot modulus can be interpreted as the moisture capacity of the material²⁵. Softening of the material, or decrease of stiffness, results in swelling of the cell wall, leading to a higher porosity to accommodate more water molecules. This results in a higher moisture capacity at higher moisture contents. As expected, the inverse of the Biot modulus of latewood is larger than the one of earlywood which indicates that latewood cells have larger moisture capacity as confirmed by experiments⁶.

The elastic Young's moduli of earlywood and latewood cells in radial and tangential directions respectively defined as $E_R = 1/S_{1111}$ and $E_T = 1/S_{2222}$, are plotted as a function

of moisture content in Fig. 4c. In both earlywood and latewood cells, $E_R > E_T$. The transverse elastic properties of earlywood are strongly anisotropic. In latewood cells the degree of anisotropy is small and the elastic Young's moduli in radial and tangential directions are close to each other. The elastic properties of thick walled latewood cells are notably larger than the ones of thin-walled earlywood cells. As anticipated, the moisture dependency of the elastic properties of the cellular tissues follows the same behavior as that of cell wall stiffness.

The above set of poroelastic properties complement the prediction of effective swelling coefficients of cellular tissues of softwood based on the poromechanical model as formulated

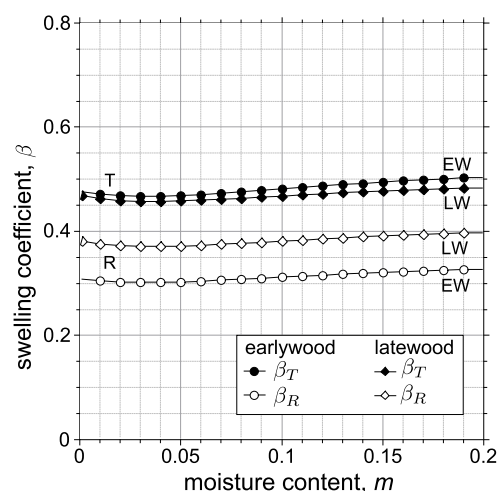


Fig. 5 Swelling coefficients of earlywood ($\phi_l = 0.64$) and latewood ($\phi_l = 0.45$) cells in radial β_R and tangential β_T directions as a function of moisture content m obtained from Eq. (6) based on poroelastic material properties presented in Fig. 4.

by Eq. (6). Fig. 5 shows the effective swelling coefficients of earlywood and latewood cells as a function of moisture content in radial ($\beta_R = \beta_{11}$) and tangential ($\beta_T = \beta_{22}$) directions. It is found that the swelling coefficients in tangential direction are bigger than in radial direction and the degree of swelling anisotropy in earlywood is larger than in latewood. The swelling anisotropy ratio β_T/β_R is almost constant for the whole range of moisture content m where, in earlywood, the ratio is about 1.6 and, in latewood, approximately equals to 1.2. The experimental values for earlywood and latewood cells of dataset B are $\beta_T/\beta_R = 1.7$ and 1.1, respectively⁶. The swelling coefficients are found to be not strongly dependent on moisture content while the elastic and Biot moduli are highly moisture dependent (Figs. 4b and c). In a typical experimental swelling curve, one can see a straight-line relationship between moisture content and swelling from zero moisture content nearly up to fiber-saturation point thus indicating constant swelling coefficients²⁶. This results can be explained considering the moisture dependent behavior of compliance and of Biot modulus. Based on the results of the proposed poromechanical model, the compliance (stiffness) increases (decreases) and the Biot modulus decreases with the increase of moisture content. Consequently, they both compensate the influence of each other on the swelling coefficient as per Eq. (6). Overall, the swelling strain exhibits a linear relationship with moisture content change.

Role of cell geometry on swelling anisotropy of tissues

The swelling properties of cellular tissues are dependent not only on the poroelastic properties of the cell walls, but also on the geometry of the cells. A parametric study is carried out to investigate the influence of the shape angle of the honeycomb unit cells on the effective swelling coefficients of earlywood and latewood tissues. Fig. 6 shows the swelling coefficients (β_R and β_T) of EW_B and LW_B at a moisture content $m = 0.12$ as a function of shape angle θ . It is found that the anisotropy in swelling coefficients is more pronounced at smaller shape angles. By increasing the shape angle, the radial and tangential poroelastic properties approach each other (not shown here for brevity reasons) and for this specific set of geometrical parameters, they exhibit a cross-over behavior. The tangential swelling coefficient β_T decreases with the increase of shape angle θ and is generally larger than β_R .

Conclusions

Motivated by experimental studies on the anisotropic swelling behavior of softwoods at the cellular scale, a double porosity poromechanical model is developed to explore the free swelling behavior of earlywood and latewood cells. The proposed method is implemented in a finite-element-based up-

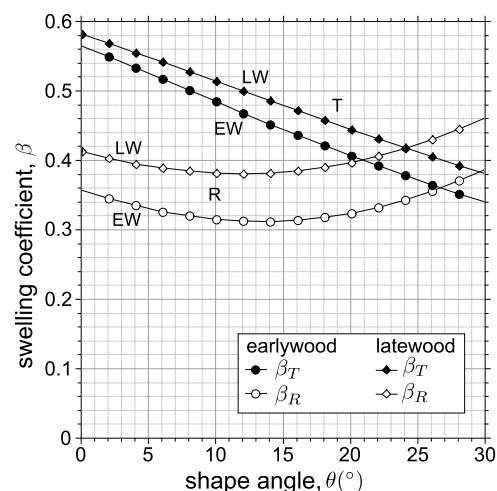


Fig. 6 Influence of shape angle of corresponding earlywood and latewood honeycomb unit cells on swelling coefficients β_R and β_T for $m = 0.12$.

scaling scheme in which the cellular tissues are simulated as periodic honeycomb unit cells. The obtained results compare well with experimental measurements. The swelling behavior results from the poroelastic interactions within the cell walls without necessity to introduce the swelling coefficients of the cell wall as inputs into the model. The proposed poromechanical model can predict several coupled physical phenomena which have been widely confirmed with experimental evidences as summarized in the following. The swelling of wood cells in tangential direction is larger than in radial direction, i.e. $\beta_T > \beta_R$, specifically for earlywood tissues. Consequently, in the RT cross-section, the degree of swelling anisotropy in earlywood is larger than one in latewood tissue. Despite the moisture dependency of the stiffness and the Biot modulus of wood cells, their cumulative interaction results in an approximately linear relationship between swelling strain and moisture content. This linear swelling behavior is also often observed by experiments. The moisture capacity of latewood cells is larger than earlywood ones. In addition to poroelastic properties, the effective swelling properties of wood cells are influenced by geometrical parameters e.g. shape angles, cell dimensions and porosity. In conclusion, the proposed model predicts the general trends accurately and gives a physical understanding of the swelling phenomenon which microscopically originates from the moisture and solid interactions within the anisotropic porous cell walls and, at cellular level, is influenced by the geometry of underlying tissues.

Acknowledgements

The synchrotron X-ray phase-contrast micro-computed tomography data was acquired at the TOMCAT beam-line of the Swiss Light Source (SLS), Paul Scherrer Institute (PSI), Villigen, Switzerland. Financial support provided by the Swiss National Science Foundation (SNSF) under grant no. 125184 is greatly acknowledged.

References

- 1 P. Fratzl and R. Weinkamer, *Progress in Materials Science*, 2007, **52**, 1263–1334.
- 2 L. J. Gibson and M. F. Ashby, *Cellular solids*, Cambridge University Press, 1997.
- 3 Z. P. Bazant, *Wood Science and Technology*, 1985, **19**, 159–177.
- 4 C. Skaar, *Wood-Water Relations*, Springer-Verlag, Berlin, Heidelberg, 1988.
- 5 D. Derome, M. Griffa, M. Koebel and J. Carmeliet, *Journal of Structural Biology*, 2011, **173**, 180–190.
- 6 A. Patera, D. Derome, M. Griffa and J. Carmeliet, *Journal of Structural Biology*, 2013, **182**, 226234.
- 7 D. Derome, A. Rafsanjani, A. Patera, J. Carmeliet and R. A. Guyer, *Philosophical Magazine*, 2012, **92**, 3680–3698.
- 8 L. G. Thygesen, E. Tang Engelund and P. Hoffmeyer, *Holzforschung*, 2010, **64**, 315–323.
- 9 T. C. Maloney and H. Paulapuro, *Journal of Pulp and Paper Science*, 1999, **25**, 430–436.
- 10 H. Qing and L. Mishnaevsky, *Computational Materials Science*, 2009, **46**, 310–320.
- 11 T. Joffe, R. C. Neagu, S. L. Bardage and E. K. Gamstedt, *Journal of Structural Biology*, 2014, **185**, 89–98.
- 12 M. A. Biot, *Journal of Applied Physics*, 1941, **12**, 155–164.
- 13 O. Coussy, *Mechanics and physics of porous solids*, Wiley, 2010.
- 14 T. Bader, K. Hofstetter, C. Hellmich and J. Eberhardsteiner, *Acta Mechanica*, 2011, **217**, 75–100.
- 15 E. Lemarchand, L. Dormieux and F.-J. Ulm, *Philosophical Transactions of the Royal Society A*, 2005, **363**, 2581–2602.
- 16 J. Carmeliet, D. Derome, M. Dressler and R. A. Guyer, *Journal of Applied Mechanics*, 2013, **80**, 020909–020909.
- 17 J. Rey and M. Vandamme, *Journal of Applied Mechanics*, 2013, **80**, 020908.
- 18 L. Dormieux, D. Kondo and F.-J. Ulm, *Microporomechanics*, John Wiley & Sons, 2006.
- 19 A. H. D. Cheng, *International Journal of Rock Mechanics and Mining Sciences*, 1997, **34**, 199–205.
- 20 R. Hill, *Journal of the Mechanics and Physics of Solids*, 1963, **11**, 357–372.
- 21 E. I. S. Flores and E. A. De Souza Neto, *Engineering Computations (Swansea, Wales)*, 2010, **27**, 551–575.
- 22 A. Rafsanjani, D. Derome, F. K. Wittel and J. Carmeliet, *Composites Science and Technology*, 2012, **72**, 744–751.
- 23 K. Persson, *PhD thesis*, 2000.
- 24 A. Rafsanjani, C. Lanvermann, P. Niemz, J. Carmeliet and D. Derome, *Composites Part A: Applied Science and Manufacturing*, 2013, **54**, 70–78.
- 25 J. Carmeliet and S. Roels, *Journal of Building Physics*, 2002, **25**, 209–237.
- 26 F. Kollmann and W. Côté, *Principles of wood science and technology I: Solid Wood*, Springer-Verlag, Berlin, 1968.